trans versus *geminal* Electron Delocalization in Tetra- and Diethynylethenes: A New Method of Analysis

Maurizio Bruschi,[a, b] Maria Grazia Giuffreda,[a] and Hans Peter Lüthi*[a]

Abstract: *trans*-Diethynylethene [(*E*)-hex-3-ene-1,5-diyne (**1a**)], *geminal*-diethynylethene [3-ethynyl-but-3-ene-1-yne (**1b**)], and tetraethynylethene [3,4-diethynyl-hex-3-ene-1,5-diyne (**2**)] are flexible molecular building blocks for π-conjugated polymers with interesting electronic and photonic properties. The type of functionalization, the length of the polymer chain, and the choice of π-conjugation pattern, play a crucial role in determining the properties of these compounds. To rationalize the impact of the different delocalization pathways in the various types of isomers (*trans* or *geminal*) on the molecular and electronic structure, a detailed theoretical investigation is presented. We develop a method based on the natural bond orbital (NBO) analysis of Weinhold, which allows one to correlate electron delocalization with molecular and electronic structure observables. The method reveals that the difference between *trans* (or through) and *geminal* (or cross) conjugation is not only due to the vertical π conjugation, but also to the in-plane σ hyperconjugation. The method is used to correlate the changes in molecular and electronic observables, such as the bond lengths or the absorption frequencies, with the electronic structure of the compounds under investigation. Moreover, this method allows us to predict how a certain substituent will affect the molecular structure and the electronic properties of a given backbone.

Keywords: ab initio calculations · conjugation · delocalization energy · molecular devices · natural bond orbital analysis

Introduction

In the recent past, π-conjugated organic polymers have been widely explored as advanced materials for electronic and photonic applications.[1] Many of these compounds have considerable flexibility, ease of processing, and the possibility of tailoring material characteristics to match a desired property. Conjugated organic molecules of multinanometer length are of particular interest in molecular electronics.[2]

The *trans*- and *geminal*-diethynylethenes **1a** and **1b** (see Scheme 1), and the tetraethynylethene **2** have been used as building blocks in the synthesis of polytriacetylenes (PTAs, $-(C{\equiv}C-CR{=}CR-C{\equiv}C)_n-$;[3] Figure 1). PTAs are a new member of a class of linearly conjugated polymers with a nonaromatic backbone, which ranges from polyacetylenes (PAs; $-(CR{=}CR)_n-$),[4] through polydiacetylenes (PDAs, $-(C{\equiv}C-CR{=}CR)_n-$),[5] to allotropic carbon polyynes ($-(C{\equiv}C)_n-$). Functionalized **1a**,**b** and **2** backbones are also extensively investigated in the design of new materials for molecular devices.[6]

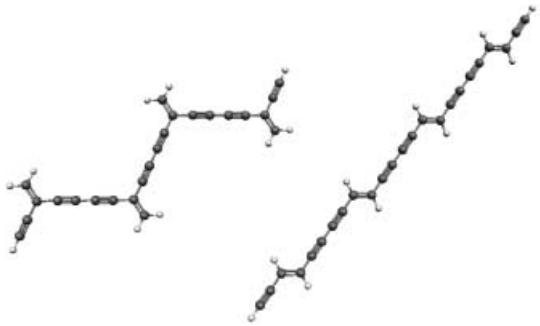

Figure 1. The *geminal* (**A**) and *trans* (**B**) PTA tetramers.

The properties of these compounds strongly depend on the type of functionalization, the length of the polymer chain, and the kind of π-conjugation patterns or π-delocalization pathways supported by these structures. A detailed knowledge of electron delocalization and its impact on the parent compounds **1a**,**b** and **2** is therefore important for the rational optimization of the properties of these linearly conjugated polymers.

[a] Dr. H. P. Lüthi, M. Bruschi, Dr. M. G. Giuffreda
Laboratorium für Physikalische Chemie
ETH Hönggerberg, HCI
8093 Zürich (Switzerland)
Fax: (+41) 16-321615
E-mail: luethi@igc.phys.chem.ethz.ch

[b] M. Bruschi
Current address: Department of Environmental Science
Università degli Studi di Milano-Bicocca
Piazza delle Scienze 1, Milan (Italy)

0947-6539/02/0818-4216 $ 20.00+.50/0 *Chem. Eur. J.* **2002**, *8*, No. 18

The electron delocalization can be expressed as the interaction between occupied fragment molecular orbitals (MOs) in one part of the molecule with specific unoccupied fragment MOs in another part of the molecule. According to this scheme, the electron delocalization can be interpreted as an intramolecular donor–acceptor interaction in which the electron density is transferred from occupied to unoccupied orbitals. This definition can be applied for both the π delocalization (or conjugation) and σ delocalization (or conjugation). In this work we will use the term delocalization to indicate all types of donor–acceptor interactions.

The natural bond orbital (NBO) theory developed by Weinhold et al.[7] provides a very useful formalism to study electron delocalization. In the NBO analysis, the delocalized (canonical) molecular orbitals are transformed into localized one-center (core orbitals and lone pairs) and two-center (the NBOs) orbitals. Hence, the total electron density is represented as far as possible by localized orbitals; this allows us to describe the molecules in terms of localized Lewis-type structures. For the conjugated systems, this picture is obviously not fully adequate. In the NBO analysis, deviations from idealized Lewis structures due to conjugation are represented as donor–acceptor interactions of localized bonds or lone pairs with antibonding orbitals ($lp \rightarrow \pi^*$ and $\pi \rightarrow \pi^*$). The delocalization results in lower occupancies of the localized bonds and lone pairs, and in larger occupancies of the antibonding orbitals. On the other hand, the delocalization energies can be determined by deletion of some or all the antibonding orbitals, followed by diagonalization of the resulting NBO Fock matrix in the reduced orbital space. Thus, the NBO analysis can be used to examine delocalization effects in molecular systems in a semiquantitative way.

The same deletion procedure has been used by von Schleyer et al.[8] to investigate the hyperconjugation effects in many molecular systems. An application of the NBO theory on benzene reveals that the deletion of the π* orbitals corresponding to the three Kekulé double bonds results in a delocalization energy ($E\pi_{del}$) of 147 kcal mol^{-1}.[9] This value is very high compared to the generally accepted value of 36 kcal mol^{-1} for the resonance energy of benzene;[10] however, it is similar to the excitation energy obtained from the lowest $\pi-\pi^*$ transition in the UV spectrum. More recently, Peyerimhoff et al.[11] have introduced a block-localized wave function (BLW) method in which the wave function is relaxed at the level of the Lewis structures. This should avoid the possible overestimation of the NBO delocalization energies evaluated at the SCF level without relaxation of the electronic structures from the Lewis representation. The method has been applied to compute the resonance stabilization of the allyl cation and the hyperconjugation effects in propene. The predicted delocalization energies are less than half of those calculated using the NBO approach.

Herein we develop a new method based on the NBO theory to study the electronic structures of **1a**,**b** and **2** (hereafter referred to as reference or parent molecules). The resulting parameters will be correlated with observables such as molecular geometries and excitation energies.

In the Results and Discussion, a detailed description of the method is presented and discussed. The molecular structures of **1a**,**b** and **2** are then analyzed with particular attention to the differences between the cross- and through-delocalization pathways. In fact, it is well established that the degree of bond length alternation (BLA) strongly correlates with the extent of electron delocalization.[12] Hence, the comparison of the molecular geometries of **1a**,**b** and **2** should give qualitative information about the differences of electron delocalization. To exclude artifacts in the data used for the analysis, it is important to study in great detail the dependence of the molecular structures on the level of theory applied. Furthermore, in this section we also give theoretical values of some important electronic properties such as electron affinities, ionization potentials, and first allowed excitation energies. The proposed method is then applied to our reference molecules, and an analysis of the differences in delocalization energies between the cross- and through-conjugation pathways is presented. The electron delocalization is also discussed in terms of changes in occupation numbers of antibonding orbitals and the flow of the charge upon orbital deletion. Finally, some interesting correlations between molecular and electronic properties with electron delocalization are also illustrated and discussed. The results from this work should give useful guidelines for the rational design of this class of materials.

Results and Discussion

Analysis of the electron delocalization

Description of the method of analysis: The method developed for the interpretation of the delocalization in the reference compounds is based on the NBO analysis of Weinhold.[7] We use NBOs and compute delocalization energies and changes in orbital occupancies to determine differences between these quantities for the set of molecules considered here. The delocalization energies and fluctuations in orbital occupancies are determined by deletion of (carefully) selected orbitals and recomputation of the energy in the reduced orbital space.

In the NBO analysis, the orbitals are labeled according to the types, that is, core, lone pair, bonding, antibonding, and Rydberg. In the allotropic π-conjugated carbon compounds such as **1a**,**b** or **2**, there are no lone pairs, and the bonding and antibonding orbitals can be split into σ, σ*, π, and π* orbitals. The π orbitals can be further reduced into a component perpendicular to the molecular plane ($\pi_\perp$) and a component in the molecular plane ($\pi_\parallel$) for both the bonding and antibonding orbitals.

The deletion of all the antibonding orbitals and the recomputation of the energy give a measure of the total delocalization energy. The difference in the delocalization energy (ΔE_{del}) computed for a pair of isomers A and B should be exactly equal to the difference of their total energies (ΔE_{tot}) as long as there are no contributions from steric strain or from the error introduced by comparison of energies determined using nonidentical orbital spaces. Ignoring the latter term for the time being, we may therefore arrive at Equation (1) in which ΔE_{del}, ΔE_{tot}, and ΔE_{strain} are the

$$\Delta E_{del} = \Delta E_{tot} - \Delta E_{strain} \quad (1)$$

  0947-6539/02/0818-4217 $ 20.00+.50/0

difference between A and B in delocalization, total, and strain energies, respectively. For the compounds studied, we can assume that ΔE_{strain} is very small compared to ΔE_{del} and can therefore be neglected.

At this point, E_{del} can be broken down into two contributions [Eq. (2)] in which E_σ and E_π take into account the delocalization due to the σ and π orbitals, respectively.

$$E_{del} = E_\sigma + E_\pi \quad (2)$$

The possible contributions of the Rydberg orbitals are of little importance in the present context and can therefore be ignored. Since the in-plane π orbitals ($\pi_\parallel$) of the molecules considered here are allowed to interact with the σ framework but not with the perpendicular orbitals ($\pi_\perp$), we arrive at Equation (3) in which $E\sigma_\parallel$ is defined by Equation (4).

$$E_{del} = E\sigma_\parallel + E\pi_\perp \quad (3)$$

$$E\sigma_\parallel = E\sigma + E\pi_\parallel \quad (4)$$

Equation (3) can be further expanded to include contributions from individual localized orbitals. However, in this case we will be confronted with nonadditivity problems due to the orbital interactions, and it is not clear whether such an analysis gives more information than Equation (3). In the present context we will look at the contributions of the individual orbitals to the differences in the delocalization energies. Moreover, our attention will also be focused on local features such as differences in the bond lengths.

Following the same procedure, we will also study the change in orbital occupancies upon deletion of antibonding (acceptor) orbitals. The deletion of an acceptor orbital followed by recomputation of the new energies in the reduced space gives important qualitative information about the flow of charge (or relaxation) associated with the disablement of a certain delocalization pathway. This approach is equivalent to the one introduced above, except that now we are tracking changes in population rather than changes in delocalization energies.

Discussion and validation of the method of analysis: All the structures considered in the present study are shown in Scheme 1. Moreover, for the reference molecules, **1a**,**b** and **2**, and for **3b**, the atom labeling is also provided in Scheme 2. For all these molecular systems, the additivity in Equations (1) and (3) is well observed. For the pair of isomers **1a** and **1b**, the difference in total delocalization energies ΔE_{del} calculated by deleting all the antibonding orbitals at the same time, and the difference in total energies ΔE_{tot} are within 0.6 kcal mol^{-1} using orbitals optimized at the B3LYP/6-31G** level of theory (see Table 7 for details). For this and later comparisons, we assume that the difference in strain (ΔE_{strain}) between the two isomers is zero. It is also noteworthy that when ΔE_{del} is calculated from Equation (3), the deviation in Equation (1) is still within 0.5 kcal mol^{-1}.

Another very important consideration is the dependence of the method on the level of theory used to calculate the energies and NBOs. There are no general rules to define how NBOs should be generated, and therefore the potential impact of the choice of the level of theory on the NBOs and the method proposed has to be carefully analyzed in each application. For the compounds studied, we actually observe patterns in the analysis of the charge and energy delocaliza-

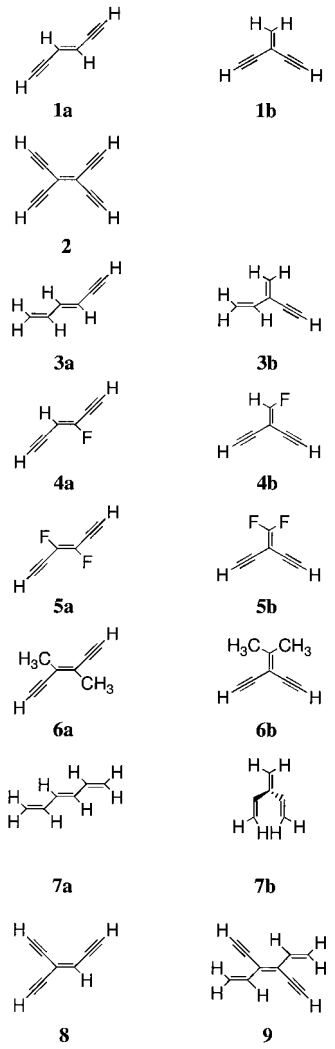

Scheme 1. The π-conjugated systems studied in the present work.

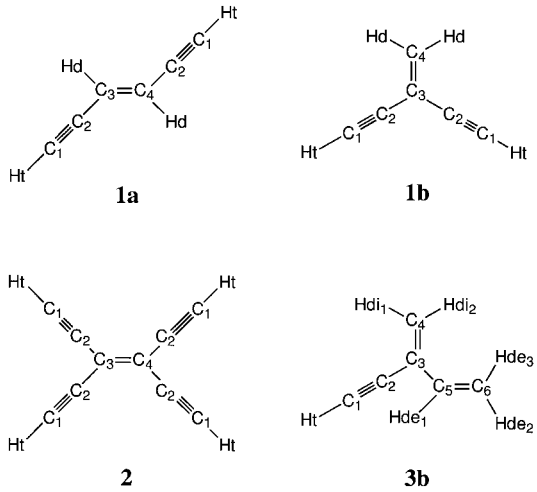

Scheme 2. Details of atom labeling used in the molecular systems **1a**,**b**, **2**, and **3b**.

0947-6539/02/0818-4218 $ 20.00+.50/0 *Chem. Eur. J.* **2002**, *8*, No. 18

tions, which are due to the systematic errors of the Hartree–Fock and the B3LYP methods. For example, when we used the Hartree–Fock orbitals and energies, the computed π delocalization energies are about 20% lower than those obtained at the B3LYP level. This is in agreement with the general observation that the Hartree–Fock method has a tendency to overlocalize π orbitals in polyenes, whereas the B3LYP method has the opposite tendency.[13] However, the differences between the delocalization energies are usually very similar.

Application of the method in the present context: The application of this method consists of a two-step procedure. Firstly, all the antibonding orbitals are deleted and the energy is recomputed in the reduced orbital space. The difference between the SCF energies calculated from the full and reduced orbital space gives the 'total delocalization energy' and corresponds to E_{del}. In the next step, the delocalization energy is split into π and σ contributions by deleting all π* orbitals perpendicular to the molecular plane and all the σ* and π* orbitals in the molecular plane, respectively. These two energies correspond to the $E\pi^*_{\perp}$ and $E\sigma^*_{\parallel}$ of Equation (3). The sum of $E\pi^*_{\perp}$ and $E\sigma^*_{\parallel}$ is labeled $E_{\pi+\sigma}$. Finally, the delocalization energies are broken down into orbital contributions for each type of bond. The deleted π* antibonding orbitals are labeled according to the bond they are associated with, that is, π^*_D, π^*_T, and $\pi^*_{\parallel}$ correspond to the π* orbitals of the C=C bonds and the vertical and in-plane C≡C bonds in **1a**,**b** and **2**. For the σ backbone, σ^*_D, σ^*_S, σ^*_T, σ^*_{Hd}, and σ^*_{Ht} correspond to the σ antibonding orbitals of the C=C, C–C, C≡C, =C–H, and ≡C–H bonds, respectively. The energy obtained from the sum of all the orbital contributions is labeled $E_{\Sigma orb}$.

Once again, it should be stressed that our interest is focused on *delocalization energy differences* between a pair of isomers, rather than on *absolute delocalization energies*.

Molecular and electronic observables: In this section we report on the experimental and computed data that will be used for the analysis of the delocalization in these compounds.

Molecular structures: experimental data: To the best of our knowledge there have been no experimental studies on the structures of the parent compounds **1a** and **1b**. On the other hand, the structures of some derivatives of **2** have been determined by X-ray diffraction experiments.[14, 15] However, these structures appear to be strongly influenced by crystal packing forces resulting in two short and two long C–C bonds as well as two short and two long C≡C bonds. The central C=C bond range from 1.324 to 1.369 Å in the different derivatives. Given the uncertainty caused by the solid-state determination, these experimental geometries do not appear suitable for comparison with theoretical (gas-phase) geometry determination. Until now, only a few theoretical studies on **1a**,**b** and **2** have been published.[16, 17]

The molecular structure of the 2-ethynyl-1,3-butadiene (**3b**, Schemes 1 and 2) has been determined experimentally using a gas-phase electron diffraction technique.[18] For this reason, a calibration of the methods can be provided by comparison of the experimental geometry of **3b** with the geometries obtained at different levels of theory. Upon inspection of the results, it appears that the B3LYP functional combined with the 6-31G** basis set gives the best agreement with the experimental values and will therefore be extensively used in the present study (see computational methods for further discussion). The geometrical parameters of **3b** calculated at different levels of theory are shown in Table 1.

***geminal*-Diethynylethene (1b)**: The computed bond lengths and bond angles of **1a**,**b** and **2** are listed in Table 2. The structure **3b** is similar to **1b** with the exception that in the former an ethynyl group has been replaced by a vinyl group. On comparison of these two molecules, it was noticed that the bond lengths remain practically unchanged. It appears, therefore, that there is no effect on the structure of the H_2C=C–C≡CH moiety when an ethynyl group is replaced with a vinyl group in a cross-conjugated way.

***trans*-Diethynylethene (1a)**: A comparison of the *trans* and *geminal* isomers reveals some interesting features. At the

Table 1. The geometrical parameters [Å and °] of **3b** calculated at different levels of theory (see Scheme 2 for atom labels).

	HF/6–31G**	MP2/6–31G**	MP3/6–31G**	MP4(SDQ)/6–31G**	B3LYP/6–31G**	Experiment[a]
C3=C4	1.328	1.352	1.346	1.348	1.350	1.357
C2–C3	1.447	1.436	1.444	1.445	1.435	1.433
C1≡C2	1.188	1.223	1.209	1.215	1.210	1.215
C1–Ht	1.057	1.067	1.062	1.063	1.065	1.062
C3–C5	1.478	1.470	1.475	1.476	1.474	1.481
C5=C6	1.321	1.342	1.337	1.340	1.337	1.342
C–Hde1	1.075	1.067	1.083	1.085	1.088	1.091
C–Hde2	1.075	1.067	1.080	1.081	1.086	1.091
C–Hde3	1.075	1.067	1.079	1.080	1.085	1.091
C4–Hdi1	1.075	1.067	1.078	1.080	1.084	1.091
C4–Hdi2	1.075	1.067	1.080	1.081	1.085	1.091
C4=C3–C5	121.45	121.28	121.47	121.45	121.13	122.0
C3–C5=C6	125.70	124.59	124.73	124.95	125.45	126.0
C4=C3–C2	120.07	120.31	120.06	120.24	120.37	120.0
C5=C6–Hde2	119.80	120.98	121.50	121.59	121.48	120.0
C3=C4–Hdi1	121.64	121.47	121.60	121.64	121.66	123.0
C3–C2≡C1	179.71	178.48	179.01	179.01	179.10	180.0

[a] Ref. [18].

Table 2. The geometrical parameters [Å and °] of **1a**, **1b**, and **2** calculated at different levels of theory (see Scheme 2 for atom labels).

	HF/6–31G**			MP2/6–31G**			MP3/6–31G**			MP4(SDQ)/6–31G**			B3LYP/6–31G**		
	1b	**1a**	**2**	**1b**	**1a**	**2**	**1b**	**1a**	**2**	**1b**	**1a**	**2**	**1b**	**1a**	**2**
C3=C4	1.327	1.328	1.345	1.352	1.355	1.381	1.346	1.347	1.367	1.349	1.349	1.369	1.351	1.354	1.384
C2–C3	1.445	1.435	1.438	1.436	1.423	1.426	1.444	1.432	1.437	1.444	1.433	1.436	1.435	1.417	1.424
C1≡C2	1.187	1.189	1.187	1.223	1.224	1.225	1.208	1.209	1.207	1.215	1.216	1.216	1.209	1.212	1.210
≡C1–Ht	1.057	1.057	1.057	1.063	1.063	1.063	1.062	1.061	1.062	1.063	1.063	1.063	1.065	1.065	1.066
=C4–Hd	1.074	1.076		1.080	1.084		1.078	1.081		1.080	1.083		1.084	1.088	
C4=C3–C2	121.60	123.04	121.9	121.54	122.82	121.03	121.47	122.69	121.49	121.62	122.87	121.4	121.65	123.70	121.5
C3–C2≡C1	179.48	178.70	178.0	179.55	178.61	178.90	179.37	178.49	178.46	179.64	178.58	178.5	178.82	178.03	177.7
C2≡C1–Ht	179.91	179.60	179.4	179.92	179.25	179.79	179.83	179.30	179.56	179.93	179.33	179.6	179.60	179.20	179.3
C3=C4–Hd	120.91	120.24		120.60	119.33		120.76	119.94		120.79	119.81		120.80	119.26	

B3LYP/6–31G** level it has been found that the C=C and C≡C bond lengths in the *trans* isomer **1a** are 0.003 Å longer than those in **1b**. To study the impact of the π delocalization on the C=C bond length, the ethylene has been taken as reference. By comparing the C=C bond lengths obtained for ethylene (1.330 Å) and for the isomers **1a** (1.354 Å) and **1b** (1.351 Å), we found an increase of this bond length of 0.024 Å for **1a** and 0.021 Å for **1b**. These variations are rather large with respect to the 0.003 Å observed between **1a** and **1b**. The effect of the electron delocalization on the C=C bond length appears to be very similar for **1b** and **1a** despite the different delocalization pathways (through versus cross). Similar considerations apply to the C≡C bond lengths. Once again, the difference between the C≡C bond lengths of **1a** and **1b** is small compared to the elongation from the acetylene reference. Apparently, the length of the double and triple bonds is not a good hallmark for discriminating between cross and through electron delocalization in the isomers **1a** and **1b**.

In contrast to the very similar C=C and C≡C bond lengths discussed above, the single C–C bond length has the largest difference between **1b** and **1a**. At the B3LYP level, the C–C bond length in **1b** is 0.018 Å longer than that in **1a**. The origin of this difference will be further investigated below.

Tetraethynylethene (2): In general, it has been found that the most important difference between **2** and the two isomers **1a** and **1b** is a substantial lengthening of the C=C bond at all levels of theory. In particular, at the B3LYP/6–31G** level the C=C bond length of **2** is about 0.030 Å longer than the corresponding lengths in **1a** and **1b**. On the other hand, comparison of the C≡C and C–C bond lengths of **2** and **1a**, revealed that the triple bond of the former is 0.007 Å longer than that in the latter, whereas the single bond is 0.002 Å shorter. Hence, the C–C and C≡C bond lengths in **2** are in between those calculated for **1a** and **1b**.

Total energy differences (ΔE_{tot}): The computed total energy differences between the isomers **1a** and **1b** are shown in Table 3. At all levels of theory, **1a** is more stable than **1b**. The ΔE_{tot} value ranges from 2.70 (MP4) to 4.81 kcal mol^{-1} (B3LYP).

Excitation energies: The first allowed transition energies of the reference molecules computed using the geometries optimized at different levels of theory are shown in Table 4.

Table 3. The energy difference ΔE_{tot} [kcal mol^{-1}] between **1a** and **1b** calculated at different levels of theory.

	ΔE_{tot}
HF/6–31G**	3.46
B3LYP/6–31G**	4.81
MP2/6–31G**	2.95
MP3/6–31G**	3.39
MP4(SDQ)/6–31G**	2.70
MP2/cc-pVDZ	3.02
MP2/cc-pVTZ	2.76
MP2/cc-pVQZ	2.83

Table 4. The first allowed excitation energy [eV] of **1a**,**b** and **2** calculated with the ZINDO/S hamiltonian on the geometries optimized at different levels of theory.

	ZINDO//HF/6–31G**	ZINDO//B3LYP/6–31G**	ZINDO//MP2/6–31G**	Experiment[a]
1b	4.801	4.561	4.449	
1a	4.501	4.201	4.117	4.18
2	3.899	3.579	3.499	

[a] Ref. [3a].

The computed excitation energies are particularly sensitive to the molecular geometries. For the isomer **1a**, an experimental value[3a] of the first allowed transition energy is available. By comparison of the theoretical and experimental results, it has been found that the best agreement is obtained by using the structure optimized at the B3LYP/6–31G** level. The first allowed transition energy difference (ΔE_{exc}) between **1a** and **1b** is equal to 8.30 kcal mol^{-1}, whereas the differences between **2** and **1a** and **1b** are equal to 14.29 and 22.59 kcal mol^{-1}, respectively. In all cases, the HOMO → LUMO transition gives the main contribution to the excited state.

Molecular ions: The molecular structures of the anions and cations **1a**,**b** and **2** are listed in Table 5. Significant changes of the geometries are observed with respect to the neutral molecules in all the cases considered. For **1b**$^-$ it has been found that the C=C bond length is 0.079 Å longer than that in the neutral species, the C–C bond length is shortened by 0.028 Å and, finally, the C≡C bond length is lengthened by 0.025 Å. For **1a**$^-$ on the other hand, the C=C bond length increases by 0.066 Å with the respect to the neutral system,

0947-6539/02/0818-4220 $ 20.00+.50/0 *Chem. Eur. J.* **2002**, *8*, No. 18

Table 5. The geometrical parameters [Å and °] of **1a**, **1b**, and **2** anions and cations calculated at the B3LYP/6–31G** level of theory using the unrestricted formalism (see Scheme 2 for atom labels).

	Anions			Cations		
	1b$^-$	**1a**$^-$	**2**$^-$	**1b**$^+$	**1a**$^+$	**2**$^+$
C3=C4	1.430	1.420	1.450	1.406	1.401	1.439
C2–C3	1.410	1.381	1.410	1.404	1.380	1.401
C1≡C2	1.237	1.251	1.223	1.219	1.226	1.216
≡C1–Ht	1.073	1.080	1.065	1.072	1.073	1.071
=C4–Hd	1.084	1.091		1.086	1.089	
C4=C3–C2	121.45	125.49	121.51	119.88	122.08	120.51
C3–C2≡C1	174.08	173.57	176.64	179.81	178.28	179.72
C2≡C1–Ht	148.06	138.38	165.23	179.79	179.60	179.59
C3=C4–Hd	120.57	116.98		120.40	119.49	

but less than in the isomer **1b**$^-$. Furthermore, the C–C bond length decreases by 0.036 Å compared to neutral counterpart, whereas the C≡C bond length increases by 0.039 Å. For the last two bonds, the variation of the bond length is more pronounced than in the isomer **1b**$^-$. In **2**$^-$, the C=C bond length goes from 1.384 Å for the neutral system to 1.450 Å for the anion with a difference of 0.066 Å (exactly the difference observed in **1a**$^-$). Finally, the C–C bond length shortens by 0.014 Å, whereas the C≡C bond lengthens by 0.013 Å.

Despite the opposite charge of the molecules, the structural differences between the neutral molecules and the cations are similar to those described for the anions. For the positively charged species, the lengthening of the C=C and C≡C bonds is generally smaller than those in the anions, whereas the increase of the C–C bond lengths is larger.

Electron affinities and ionization potentials: The calculated adiabatic electron affinities (EAs) and ionization potentials (IPs) are shown in Table 6. A substantial difference between the EAs of the isomers **1a** and **1b** has been found by comparing the values obtained by using the BHandHLYP functional together with the 6–31G** basis set. In fact, the EA is positive for **1a** and negative for **1b**, which means that the extra electron is bound in the former and unbound in the latter. As can be easily predicted, the isomer **2** with its extended delocalization pattern has the highest EA. The difference between the EAs of **1a** and **1b** is equal to 5.17 kcal mol^{-1}, whereas those calculated between **2** and **1a** and **1b** are equal to 20.69 and 25.85 kcal mol^{-1}, respectively.

Table 6. The adiabatic electron affinities and ionization potentials [eV] of **1a**, **1b**, and **2** calculated at different levels of theory.

	1b	**1a**	**2**
	adiabatic electron affinities		
B3LYP/6–31G**//B3LYP/6–31G**	–0.489	–0.133	0.665
B3LYP/6–31+G** Bqc//B3LYP/6–31G**	0.144	0.345	1.017
BhandHLYP/6–31+G** Bqc//B3LYP/6–31G**	–0.157	0.067	0.964
	adiabatic ionization potentials		
B3LYP/6–31G**//B3LYP/6–31G**	8.549	8.301	7.309

The IPs of the reference molecules have been calculated at the B3LYP/6–31G** level of theory. The highest and lowest IPs are observed for the structures **1b** and **2**, respectively. It is important to note that the IP differences between **1a** and **1b**, and between **2** and **1a** and **1b** are equal to 5.72, 22.88, and 28.60 kcal mol^{-1}, respectively. These values are similar to the differences observed for the EAs.

Analysis of delocalization and its correlation with molecular and electronic properties: The delocalization energies have been calculated by applying the method defined above. These energies for the reference molecules have been computed at the B3LYP/6–31G** level of theory and are shown in Table 7.

The $\Delta E_{\mathrm{del}(\mathbf{1a-1b})}$ obtained by deleting all the antibonding orbitals is 5.42 kcal mol^{-1} in favor of the *trans* isomer. This is in very good agreement with the difference in stability calculated from the total energies ($\Delta E_{\mathrm{tot}(\mathbf{1a-1b})} = 4.81$ kcal mol^{-1}).

According to Equation (3), the total delocalization energy can be expressed as a sum of the two components $E\pi^*_{\perp}$ and $E\sigma^*_{\parallel}$. By this partition, it appears that the main contribution to the energy difference $\Delta E_{\mathrm{del}(\mathbf{1a-1b})}$ is due to the π conjugation, that is, $\Delta E\pi^*_{\perp(\mathbf{1a-1b})}$. In fact, as shown in Table 7, the $\Delta E\sigma^*_{\parallel(\mathbf{1a-1b})}$ is 0.35 kcal mol^{-1} in favor of the *geminal* isomer **1b**, whereas the $\Delta E\pi^*_{\perp(\mathbf{1a-1b})}$ is 5.45 kcal mol^{-1} in favor of the *trans* isomer **1a**. The sum of the $\Delta E\pi^*_{\perp}$ and $\Delta E\sigma^*_{\parallel}$, that is, $\Delta E_{\pi+\sigma(\mathbf{1a-1b})}$, is equal to 5.10 kcal mol^{-1} and matches nearly perfectly with both ΔE_{tot} and ΔE_{del}.

By inspection of the delocalization energies at the individual orbital levels, it can be noted that in the σ skeleton significant differences are observed by deleting the σ* orbitals corresponding to the C–C (σ^*_{S}) and =C–H (σ^*_{Hd}) bonds. In fact, the $E\sigma^*_{\mathrm{S}}$ calculated for the *geminal* isomer **1b** is 15.96 kcal mol^{-1} higher than that obtained for the *trans* isomer **1a**. This could also be related to the fact that the largest bond length difference between **1a** and **1b** is observed for precisely this particular bond. However, the advantage of the *geminal* isomer within the carbon σ skeleton is cancelled by the $E\sigma^*_{\mathrm{Hd}}$, which for the *trans* isomer **1a**, has been found to be 12.54 kcal mol^{-1} higher than that of the isomer **1b**. Here also, a slight difference in the =C–H bond length is observed.

Table 7. The π and σ delocalization energies [kcal mol^{-1}] of **1a**, **1b**, and **2** calculated at the B3LYP/6–31G** level. The number of deleted antibonding orbitals is shown in parenthesis.

	$E\pi^*_{\mathrm{D}}$	$E\pi^*_{\mathrm{T}}$	$E\sigma^*_{\mathrm{D}}$	$E\sigma^*_{\mathrm{S}}$	$E\sigma^*_{\mathrm{T}}$	$E\sigma^*_{\mathrm{Hd}}$	$E\sigma^*_{\mathrm{Ht}}$	$E\pi^*_{\parallel}$	$E\pi^*_{\perp}$	$E\sigma^*_{\parallel}$	$E_{\Sigma\mathrm{orb}}$	$E_{\pi+\sigma}$	E_{del}	E_{tot}
1a	28.18 (1)	33.33 (2)	14.55 (1)	42.73 (2)	47.49 (2)	20.07 (2)	16.35 (2)	13.47 (2)	53.88 (3)	158.94 (11)	216.17 (14)	212.82 (14)	213.92 (14)	
1b	23.14 (1)	29.48 (2)	14.76 (1)	58.69 (2)	46.48 (2)	7.53 (2)	16.66 (2)	10.49 (2)	48.43 (3)	159.29 (11)	207.23 (14)	207.72 (14)	208.50 (14)	
$\Delta E_{\mathbf{1a-1b}}$	**5.04**	**3.85**	**–0.21**	**–15.96**	**1.01**	**12.54**	**–0.31**	**2.98**	**5.45**	**–0.35**	**5.50**	**5.10**	**5.42**	**4.81**
2	63.69 (1)	46.42 (4)	28.44 (1)	109.51 (4)	93.28 (4)		32.37 (4)	21.47 (4)	106.12 (5)	295.54 (17)	395.18 (22)	401.66 (14)	403.07 (22)	
2-trans	63.69 (1)	29.25 (2)	28.44 (1)	56.15 (2)	46.32 (2)		16.17 (2)	10.98 (2)	82.29 (3)					
$\Delta E_{\mathbf{2trans-1a}}$	**35.51**	**–4.08**	**13.89**	**13.42**	**–1.17**		**–0.18**	**–2.49**	**28.41**					
2-gem	63.69 (1)	32.43 (2)	28.44 (1)	55.33 (2)	46.58 (2)		16.17 (2)	10.69 (2)	82.86 (3)					
$\Delta E_{\mathbf{2gem-1b}}$	**40.55**	**–2.95**	**13.68**	**–3.36**	**0.10**		**–0.49**	**0.20**	**34.43**					

  0947-6539/02/0818-4221 $ 20.00+.50/0

Another source of energy difference between the isomers **1a** and **1b** is the in-plane π* C≡C orbitals ($\pi^*_{\parallel}$). The $\Delta E\pi^*_{\parallel}$ amounts to 2.98 kcal mol^{-1} in favor of **1a**. In conclusion, the total difference in the delocalization energy is controlled by the $\pi_{\perp}$ conjugation; however, the contributions owing to the energy differences of the σ^*_S and σ^*_{Hd} orbitals are interestingly high, but due to their opposite effect they cancel each other.

At the HF level, the same considerations are still valid (data not shown). As expected, the absolute values of the π delocalization energies (E_{del}) are in general smaller to those obtained at the B3LYP/6–31G** level. Finally, this HF-inherent underestimation of the π delocalization disfavors the *trans* isomer relatively more than the *geminal* isomer.

For **2**, the number of bonding and antibonding orbitals is larger and, therefore, the computed delocalization energies are considerably higher. To obtain values directly comparable with those calculated for **1a** and **1b**, we compute delocalization energies deleting only the three $\pi^*_{\perp}$ orbitals in a *trans* or in a *geminal* arrangement. As shown in Table 7, the *trans* and *geminal* $\pi^*_{\perp}$ delocalization energies in **2** do not differ appreciably. The difference between the "*trans*" $\pi^*_{\perp}$ delocalization energy in **2** and that calculated for **1a**, that is, $\Delta E\pi^*_{\perp(\mathbf{2}trans-\mathbf{1a})}$, is equal to 28.41 kcal mol^{-1}. This value is a measure for the $\pi_{\perp}$ delocalization energy resulting from the effect of the functionalization of the **1a** backbone with two acetylenic substituents. This can be a useful tool to study the impact of the functionalization on the electron delocalization of the π-conjugated molecular systems. This issue will be addressed in a future study.

The $\pi^*_{\perp}$ delocalization energy has been further analyzed by considering the π^*_D and π^*_T contributions. Since there is only one π_D orbital in all the three systems (**1a**, **1b**, and **2**), the delocalization energy obtained by deleting the π^*_D orbital is directly comparable. The $E\pi^*_D$ calculated for **2** is more than double that calculated for the **1b** or **1a** backbones. This large increase of the $E\pi^*_D$ suggests that the two additional acetylenic arms have a strong additive effect in promoting the π delocalization. On the other hand, the $E\pi^*_T$ computed by deleting the two π^*_T orbitals in the *trans* arrangement is lower than that computed for **1a**. This suggests a less efficient back-donation from π_D into π^*_T when the two acetylenic groups are added to the *trans* diethynylethene backbone.

The method described above has also been applied to the other isomers presented in Scheme 1. E_{del}, $E\sigma^*_{\parallel}$, and $E\pi^*_{\perp}$ contributions as well as the difference in stability calculated from the total energies are provided in Table 8. For the isomers **3a**,**b**, **4a**,**b**, and **6a**,**b** the agreement between the difference in the delocalization and total energies is excellent, that is, within 1 kcal mol^{-1}. At this point, it should be noted that both the σ and π components contribute to the difference in stability. For the isomers **3a**,**b**, the $\Delta E\pi^*_{\perp}$ of 5.95 kcal mol^{-1} in favor of the *trans* isomer is mitigated by the $\Delta E\sigma^*_{\parallel}$ contribution of 2.67 kcal mol^{-1} in favor of the *geminal* isomer. Therefore, the decrease of ΔE_{tot} when comparing **3a**,**b** with **1a**,**b** is mainly due to the differences in the σ delocalization rather than in the π conjugation. In the monofluorinated isomers **4a**,**b**, both $\pi^*_{\perp}$ and $\sigma^*_{\parallel}$ components favor the *trans* isomer; however, the $\Delta E\pi^*_{\perp}$ decreases to 2.49 kcal mol^{-1}. The difluorinated compounds **5a**,**b** are the only isomers that exhibit a significant difference between ΔE_{tot} and ΔE_{del}. The *gem*-difluorinated compound **5b** is more stable than in the *trans* arrangement **5a** by 5.28 kcal mol^{-1}. The ΔE_{del} correctly predicts the inversion of the stability, but drastically overestimates the energy splitting. The origin of this discrepancy will be subject to further investigations. In sharp contrast to the molecules discussed above, the steric strain of **7b** is not negligible. In fact, the B3LYP/6-31G** predicts a nonplanar structure of C_2 symmetry ($\mathbf{7b}_{C_2}$) for **7b**, whereas at the same level the planar structure of C_{2v} symmetry ($\mathbf{7b}_{C_{2v}}$) is found to possess an imaginary frequency and, therefore, is a transition state. For this reason, a discrepancy between ΔE_{tot} and ΔE_{del} is expected. Indeed for the isomers **7a** and $\mathbf{7b}_{C_2}$, these two quantities differ by 2.73 kcal mol^{-1}. If we consider the steric strain of **7a** to be negligible, this value could be an estimation of the steric energy in $\mathbf{b}_{C_2}$. The decomposition of E_{del} into $\pi^*_{\perp}$ and $\sigma^*_{\parallel}$ reveals that the $\Delta E\pi^*_{\perp}$ of 9.31 kcal mol^{-1} in favor of the *trans* isomer is partially compensated for by the $\Delta E\sigma^*_{\parallel}$ of 4.49 kcal mol^{-1} in favor of the *geminal* compound.

A more detailed investigation of the origin of the hyperconjugative interactions leading to the σ and π delocalization can be carried out by considering the changes of the σ or π orbital occupations. The variation of the NBO occupations for **1a**,**b** and **2** are shown in Table 9. The $\pi_{\perp}$ delocalization

Table 8. The energy differences [kcal mol^{-1}] of the pair of isomers drawn in Scheme 1 and calculated at the B3LYP/6–31G** level of theory. The number of deleted antibonding orbitals is provided in parenthesis.

	$\Delta E\pi^*_{\perp}$	$\Delta E\sigma^*_{\parallel}$	$\Delta E_{\pi+\sigma}$	ΔE_{del}	ΔE_{tot}
3a–3b	5.95 (3)	–2.67 (11)	3.28 (14)	3.42 (14)	3.36
4a–4b	2.49 (3)	1.29 (11)	3.78 (14)	3.57 (14)	3.67
5a–5b	–5.85 (3)	–19.81 (11)	–25.66 (14)	–26.97 (14)	–5.28
6a–6b	–0.05 (3)	1.20 (11)	1.15 (14)	1.38 (14)	2.26
7a–7b	9.31 (3)	–4.49 (11)	4.82 (14)	4.68 (14)	7.41

Table 9. Changes in the occupation of the π and σ orbitals by deleting selected π* or σ* orbitals.

Deleted orbitals	Orbitals with changes in occupation	**1b**	**1a**	**2**
		Orbital occupation changes		
$\pi^*_{\perp}$	π_D	0.110	0.131	0.213
	π^*_D	–0.121	–0.143	–0.292
	π_T	0.061	0.079	0.085
	π^*_T	–0.056	–0.075	–0.067
σ^*_s	σ_D	0.005	0.003	0.010
	σ_{Hd}	0.010	0.001	–
	σ_T	0.007	0.007	0.008
	$\pi_{\parallel}$	0.008	0.002	0.009
	σ_S	~0.00	0.004	0.005
	σ^*_S	–0.034	–0.020	–0.030
$\pi^*_{\parallel}$	σ_D	0.009	0.010	0.016
	σ_{Hd}	0.006	0.014	–
	σ_S	0.001	~0.00	0.006
	$\pi_{\parallel}$	0.004	0.001	0.007
	$\pi^*_{\parallel}$	–0.016	–0.020	–0.016
σ^*_{Hd}	σ_D	0.001	0.001	–
	σ_S	0.004	~0.00	–
	$\pi_{\parallel}$	0.002	0.009	–
	σ^*_{Hd}	–0.006	–0.019	–

0947-6539/02/0818-4222 $ 20.00+.50/0 *Chem. Eur. J.* **2002**, *8*, No. 18

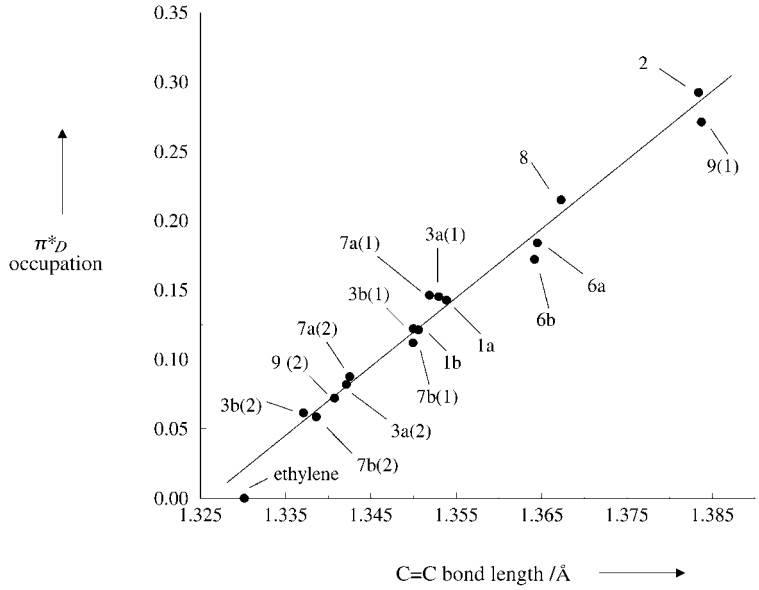

Figure 2. The π^*_D orbital occupation calculated by the NBO theory at the B3LYP/6–31G** level of theory as a function of the C=C bond lengths for the molecules represented in Scheme 1. For the molecules with different C=C bonds, the numbers in parenthesis indicates the specific C=C bond, that is, (1) is the central and (2) is the peripheral bond.

energies are easily attributed to $\pi_T \rightarrow \pi^*_D$ and $\pi_D \rightarrow \pi^*_T$ donor–acceptor interactions. When the $\pi^*_\perp$ orbitals of isomer **1b** are deleted, the electron population which moves from the π^*_D to the π_T orbital (0.121) is larger than that which moves from the π^*_T to the π_D orbital (0.110). For the isomer **1a**, a similar but more pronounced transfer is observed. Therefore, for both the molecules, there is a net increase of the π^*_D orbital occupation and a corresponding decrease of the π^*_T occupancy, which confirms that the π_T orbitals act as π donors to the central C=C bond. In compound **2**, the occupation of the π^*_D orbital is roughly double that calculated for the isomer **1a**. The addition of two acetylenic arms to the diethynylethene backbone leads to an additive effect (actually more than additive) which is reflected in the π^*_D occupation. By considering the variation of the occupation numbers of the π^*_D orbitals, the order **1b** < **1a** < **2** is determined. On the other hand, for the π^*_T orbitals, the order becomes **1b** < **2** < **1a**, which means that the $\pi_D \rightarrow \pi^*_T$ back-donation of **2** is in between that obtained for **1a** and **1b**. Finally, it is noteworthy that this behavior can be correlated to the differences of the C=C and C≡C bond lengths. Similar considerations have been observed for the σ^*_S, σ^*_{Hd}, and $\sigma^*_\parallel$ orbital occupations. In fact, the σ^*_S occupation number decreases in the order **1b** > **2** > **1a**; this agrees with the calculated $E\sigma^*_S$ and the differences in C–C bond lengths.

Several donor–acceptor interactions contribute to the occupation of the σ^*_S orbitals. For **1a,b**, the σ_{Hd} and $\pi_\parallel$ orbitals give the strongest donor contribution. However, the contributions are much lower in **1a**.

The differences in occupation of the in-plane π orbitals ($\pi^*_\parallel$) are controlled by the hyperconjugative interactions with the σ orbitals of the backbones of the molecules. The only significant difference is in a stronger donor–acceptor interaction with the σ_{Hd} orbitals. This means that the functionalization with the σ donors or acceptors should be most efficient when this functionalization is positioned at the double bond. The positioning of the σ donor/acceptor at the triple bond will be less effective.

As outlined above, a strong correlation between the π* and σ* orbital occupations with the corresponding bond length distances can be observed. To further investigate this critical point, the occupation of the antibonding orbitals of all the molecules represented in Scheme 1 (with the exception of the difluorinated isomers **5a**,**b**) has been considered. The correlation between the π^*_D occupation numbers and the C=C bond lengths is shown in Figure 2. A straight line is obtained with a correlation coefficient of 0.990. However, a similar correlation is not found for the σ^*_D occupation numbers. This could suggest that despite the differences in σ^*_D occupation numbers, the C=C bond lengths depend only (or mainly) on the occupation of the π* orbitals.

As shown in Figure 3, a linear correlation between the bond lengths and the π^*_T occupation is also observed for the C≡C bond. Once again, a similar correlation is not found when σ^*_T or $\pi^*_\parallel$ occupations are plotted against the corresponding bond lengths. It is noteworthy that the σ^*_S occupation numbers correlate sufficiently well with the C–C bond lengths as displayed in (Figure 4); this suggests that besides the π conjugation, the hyperconjugative delocalization is also relevant in the C–C bond length difference.

Considering the first allowed excitation energies (ΔE_{exc}) of the isomers **1a** and **1b**, it appears that the comparison with the $\Delta E\pi^*_\perp$ is rather satisfactory; in fact, they only differ by 2.88 kcal mol^{-1}. This correlation also exists for the other pairs of isomers considered (Figure 5). The computed ΔE_{exc} are systematically 2–3 kcal mol^{-1} higher than the $\Delta E\pi^*_\perp$. The origin of this correlation is not yet fully understood.

For the anions and cations of **1a**,**b** and **2**, the differences in the bond lengths can be interpreted on the basis of the calculated atomic spin densities shown in Table 10. In **1b**$^-$, the unpaired electron is highly localized on the C4 atom (see Scheme 2 for atom labels). A small "fraction" of the electron is at the C1 position, whereas the C2 and C3 atoms exhibit a negligible spin density. In **1a**$^-$, the atomic spin densities indicate that the unpaired electron is more delocalized along the carbon backbone. In particular, the spin density is high on the C1 (0.233) and C3 (0.321) atoms and, as in **1b**$^-$, it is negligible at the C2 atoms. The spin density of **2**$^-$ is comparable to that of **1a**$^-$; however, it increases on the two central atoms (C3 and C4) and decreases on the C1 atoms. The spin densities of the cations are similar to those already discussed for the anions (see Table 10).

  0947-6539/02/0818-4223 $ 20.00+.50/0

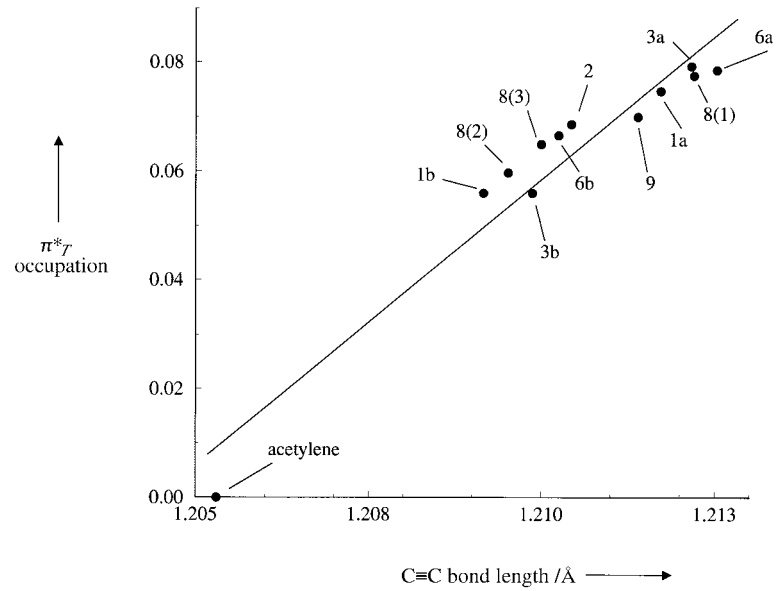

Figure 3. The π^*_T orbital occupation calculated by the NBO theory at the B3LYP/6–31G** level of theory as function of the of C≡C bond lengths for the molecules represented in Scheme 1. For **8**, the three nonequivalent C≡C bonds are indicated with the numbers in parenthesis: (1) stands for the C≡C bond on the right in Scheme 2, (2) stands for the C≡C bond at the lower left, and (3) stands for the C≡C bond at the upper left.

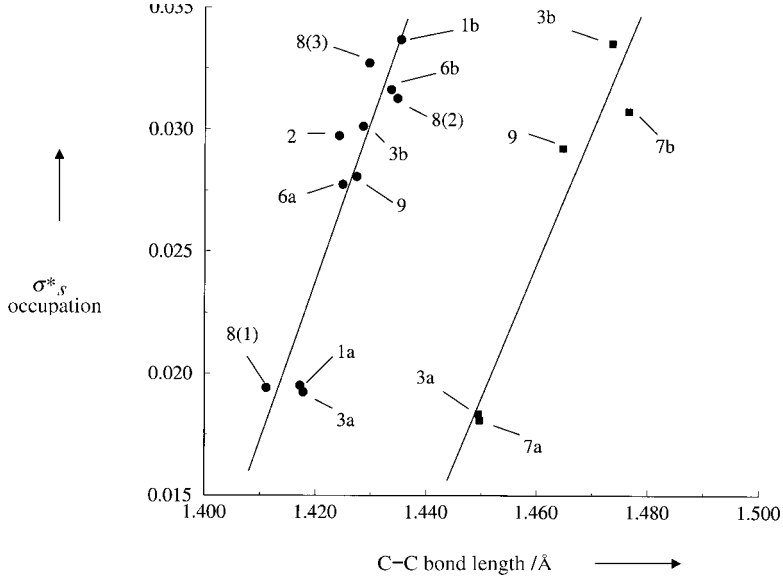

Figure 4. The σ^*_s orbital occupation calculated by the NBO theory at the B3LYP/6–31G** level of theory as function of the C–C bond lengths for the molecules represented in Scheme 1. The C–C bonds which are in between C=C and C≡C bonds are indicated by ●, whereas with C–C bonds which are in between two C=C bonds are indicted by ■. For **8**, the three nonequivalent C–C bonds are indicated with the numbers in parenthesis: (1) stands for the C–C bond on the right in Scheme 2, (2) stands for the C–C bond on the lower left, and (3) stands for the C–C bond on the upper left.

Table 10. The total atomic spin densities of the anions and cations **1a**, **1b**, and **2** calculated at the B3LYP/6–31G** level of theory using the unrestricted formalism (see Scheme 2 for atom labels).

	Anions			Cations		
	1b$^-$	**1a**$^-$	**2**$^-$	**1b**$^+$	**1a**$^+$	**2**$^+$
C4	0.728			0.569		
C3	0.038	0.233	0.268	0.045	0.209	0.208
C2	– 0.006	– 0.057	– 0.096	– 0.006	– 0.070	– 0.071
C1	0.151	0.321	0.217	0.231	0.383	0.225
Ht	0.008	0.017	– 0.006	– 0.024	– 0.009	– 0.008
Hd	– 0.036	– 0.014		– 0.008	– 0.014	

The electronic structure of the anions and cations can also be interpreted by the NBO theory. The NBO theory of an unrestricted system analyzes separately the α and β density matrix in two different sets of natural orbitals. A schematic representation of the α and β densities at the NBO level of theory is shown in Figure 6. The analysis of the β density of **1b**$^-$ reveals that the unpaired electron is localized on the C4 and C1 atoms, whereas in **1a**$^-$ the electron is localized on the two C1 atoms. Also in **2**$^-$, the unpaired electron is localized on the two equivalent C1 atoms. It is possible to explain the differences in the bond lengths from this NBO picture. In fact, in **1b**$^-$ the extra electron is localized on the C4 atom in the p_z orbital perpendicular to the molecular plane. This results in a reduction of the C=C bond order and a corresponding elongation of the bond. In **1a**$^-$, the extra electron is localized at the C1-position resulting in a larger elongation of the C≡C bond and a shorter elongation of the C=C bond with respect to **1b**$^-$. Finally, in **2**$^-$, the extra electron has two more acetylenic arms to be delocalized on, and the effect on all the bond lengths is therefore rather small.

Conclusion

Herein we present a method to analyze electron delocalization in π-conjugated organic compounds such as **1a**,**b** and **2**. The method is not designed to give absolute values for delocalization energies, but is built to reproduce differences between structural isomers or between backbones with different functionalization. These differences can be correlated with structural features such as changes in bond length. It is also possible to near-quantitatively predict shifts in the electronic excitation energies based on the comparison of conjugation patterns.

With regard to its predictive power, we demonstrate that the method not only allows us to study the impact of a specific donor, acceptor, or spacer, but it also helps to identify their location on the backbone which is most sensitive to the action

0947-6539/02/0818-4224 $ 20.00+.50/0 *Chem. Eur. J.* **2002**, *8*, No. 18

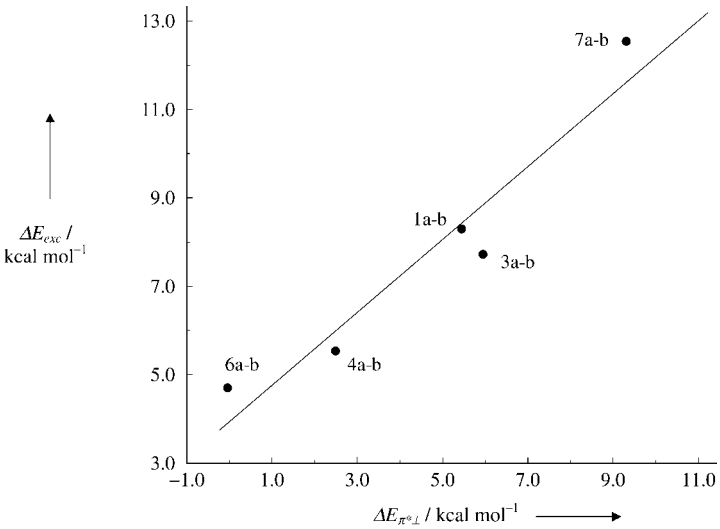

Figure 5. The calculated ΔE_{exc} between the *trans* and *geminal* isomers as function of the corresponding $\Delta E\pi_{\perp}$.

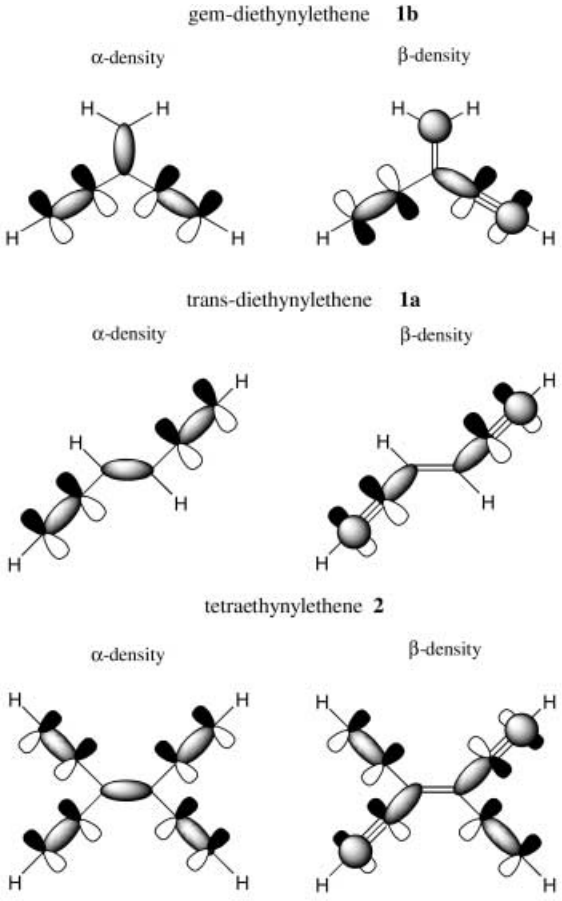

Figure 6. Schematic picture of the α and β electron density of the localized NBO orbitals for **1a**$^-$, **1b**$^-$, and **2**$^-$.

of a substituent. In this particular context, the idea of splitting the electron delocalization into vertical and parallel components has proved to be very useful.

By applying the method to the isomers **1a** and **1b**, we found that the difference in stability between the cross- and through-conjugation is controlled by the vertical π delocalization, whereas the σ delocalization plays a very minor role. However, the analysis of all the other compounds shows that the σ delocalization cannot be neglected. In fact, it is often used as a way to discriminate between *geminal* and *trans* conjugation. This is confirmed by the significant differences in the σ delocalization at the individual orbital level in **1a** and **1b**.

The importance of the σ delocalization is also supported by the fact that the largest structural differences between *trans* and *geminal* isomers are not in the π bond lengths but rather in the σ bond lengths. In fact, in the *geminal* isomers the =C–C σ bonds are consistently longer than those in the *trans* isomers.

The *geminal*–*trans* delocalization energy gap is reduced in the isomer **2** relative to **1a**,**b**, as confirmed by the fact that the C–C and C≡C bond lengths fall in between those of **1a** and **1b**. Furthermore, the two acetylenic substituents act as strong π donors causing a significant increase of the central C=C bond length.

Computational Methods

The full geometry optimizations of **3b**, **1a**,**b**, and **2** have been performed by using density functional (DFT) and ab initio approaches. In the ab initio calculations, the electron correlation has been taken into account by using the Moller–Plesset (MP) perturbation theory. Calculations at the second (MP2), third (MP3), and fourth (MP4 without triple excitation) orders have been performed by using the 6–31G** basis set of Gaussian orbitals.[19] Moreover, the basis set convergence has been checked for **1a**,**b** at the MP2 level by using the Dunning correlation consistent basis sets of double, triple, and quadruple zeta quality.[20] For the DFT calculations,[21] the Becke three-parameters Lee–Yang–Parr (B3LYP) hybrid functional,[22] consisting of the Becke's exchange functional[23] and Lee, Yang, and Parr's correlation functional,[24] has been used together with the 6–31G** basis set. All the structure optimizations have been performed in the planar arrangement, which are shown to be pure minima by vibrational analysis. In order to match a sufficient accuracy of the geometrical parameters, we have adopted a convergence threshold of 5.0×10^{-5} Hartree Bohr^{-1} or Hartree Rad^{-1}.

The most appropriate level of theory for the geometry optimizations is selected by comparing the computed geometrical parameters of **3b** with the experimental gas-phase electron diffraction structure.[18] The theoretical and experimental parameters are reported in Table 1. At the Hartree–Fock (HF) level, as observed in similar studies (see for example ref. [25]), the C3=C4 and C1≡C2 bond lengths are underestimated by 0.029 and 0.027 Å, respectively. When correlation is taken into account, both the DFT and ab initio results agree well with the experimental results. In the worst case, that is, MP3, the C3=C4 bond length is underestimated by 0.011 Å. Similar arguments hold for the C5=C6 bond lengths. All the correlated methods give values very close to the experimental results, in fact the difference never exceeds 0.005 Å. For the C2–C3 bond length, the MP2 and B3LYP models are in perfect agreement with the experiment, whereas at the MP3 and MP4 levels, this bond length is overestimated by about 0.010 Å. All the methods compare reasonably well with the experiment with the exception of the HF results. In particular, the B3LYP and MP2 methods predict very similar geometries and they give the best agreement with the experiment. The calculations performed at the MP2 level using the correlated consistent basis set of Dunning up to the quadruple zeta quality (data not shown) indicate that the C≡C bond length, for which with the 6–31G** basis there is the largest difference between MP2 and B3LYP approaches (0.013 Å), converges to the B3LYP value. Moreover, it should be noted that, despite the differences in the absolute values of the bond lengths calculated at different levels of theory, the changes between the *geminal* and the *trans* molecules are always very similar.

  0947-6539/02/0818-4225 $ 20.00+.50/0

The excitation energies have been computed by using the semiempirical intermediate-neglected differential overlap (INDO/S) hamiltonian parametrized by Zerner et al.[26] on previously optimized geometries. The active space contained all the virtual and occupied orbitals (full single CI calculation).

The adiabatic electron affinities (EAs) and ionization potentials (IPs) have been calculated as differences between the energies of the neutral and ionic species at the equilibrium geometries. The B3LYP/6–31G** level of theory has been used for all structure optimizations. The open shell species have been calculated by using the unrestricted formalism. The neutral molecules were optimized (as specified above) in the planar arrangement, whereas the anions were optimized in a lower nonplanar symmetry. In fact, the vibrational analysis reveals that the planar geometries are stationary points with two imaginary frequencies corresponding to a symmetric or asymmetric bend out-of-plane of the terminal hydrogens. The optimization of the structures in these two configurations leads to two genuine minima with an energy difference lower than 0.1 kcal mol^{-1}. The cations have been optimized in the planar geometries. The vibrational analysis confirmed that these are pure minima.

For the anions at the equilibrium geometries, single point energy calculations at the B3LYP/6–31+G** and BHandHLYP/6-31+G** levels have been performed. The addition of diffuse functions, however, leads to strong linear dependence in the basis set. This is due to the large overlap of the diffuse functions centered on the acetylenic carbon atoms. To avoid this problem, the acetylenic systems have been described by using bond-centered diffuse functions. The level of theory applied is represented as follows: B3LYP/6–31+G**//B3LYP/6–31G** for general atoms, and B3LYP/6–31+G**(Bq)//B3LYP/6–31G**, in which Bq stands for a single set of diffuse functions centered on the acetylenic bonds. Benchmark calculations on small molecular systems[27] and by us on nitrobenzenes (data not shown) have demonstrated that the BHandHLYP functional[28] in the framework of the DFT theory gives the best result. However, the B3LYP functional generally overestimates the EAs.

All the calculations have been performed with the Gaussian 98 package.[29] The natural bond orbital analysis has been performed with the program NBO 3.1[30] as implemented in Gaussian 98.

Acknowledgement

This research project was supported by the Swiss National Science Foundation through grants 20–61893.00 and 20–54065.98. The authors also acknowledge inspiring discussions with F. Diederich and co-workers. M.B. would also like to thank P. Fantucci for critical comments and discussions.

[1] a) *Electronic Properties of Conjugated Polymers III: Basic Models and Applications* (Eds: H. Kuzmani, M. Mehring, S. Roth), Springer, Berlin **1989**; b) J. S. Miller, *Adv. Mater.* **1993**, *5*, 671–676; c) *Handbook of Conducting Polymers Vols. 1, 2* (Ed: T. A. Skotheim) Dekker, New York **1986**; d) *Conjugated Polymers and Related Materials. The Interconnection of Chemical and Electronic Structure* (Eds: W. R. Salaneck, I. Lundström, B. Ränby), Oxford University Press, Oxford, **1993**; e) M. Liphardt, A. Goonesekera, B. E. Jones, S. Ducharme, J. M. Takacs, L. Zhang, *Science* **1994**, *263*, 367–369; f) N. C. Greenham, S. C. Moratti, D. D. C. Bradley, R. H. Friend, A. B. Holmes, *Nature* **1993**, *365*, 628–630; g) A. Buckley, *Adv. Mater.* **1992**, *4*, 153–158; h) H. S. Nalwa, *Adv. Mater.* **1993**, *5*, 341–358.

[2] a) D. L. Pearson, J. S. Schumm, J. M. Tour, *Macromolecules* **1994**, *27*, 2348–2350; b) P. Seta, E. Bienvenue, *Mol. Electron Devices* **1994**, *3*, 59–78; c) L. Jones II, D. L. Pearson, J. S. Schumm, J. M. Tour, *Pure Appl. Chem.* **1996**, *68*, 145–148; d) J. M. Tour, *Chem. Rev.* **1996**, *96*, 537–553; e) M. D. Ward, *Chem. Ind.* (London) **1996**, *15*, 568–573. f) T. Bartik, B. Bartik, M. Brady, R. Dembinski, J. A. Gladsyz, *Angew. Chem.* **1996**, *108,* 467–469; *Angew. Chem. Int. Ed. Engl.* **1996**, *35*, 414–417; g) J. S. Schumm, D. L. Pearson, J. M. Tour, *Angew. Chem.* **1994**, *106*, 1445–1448; *Angew. Chem. Int. Ed. Engl.* **1994**, *33*, 1360–1363; h) R. H. Grubbs, D. Kratz, *Chem. Ber.* **1993**, *126*, 149–157.

[3] a) M. Schreiber, J. Anthony, F. Diederich, M. E. Spahr, R. Nesper, M. Hubrich, F. Bommeli, L. Degiorgi, P. Wachter, P. Kaatz, C. Bosshard, P. Günter, M. Colussi, U. W. Suter, C. Boudon, J.-P. Gisselbrecht, M. Gross, *Adv. Mater.* **1994**, *6*, 786–790; b) M. Schreiber, R. R. Tykwinski, F. Diederich, R. Spreiter, U. Gubler, C. Bosshard, I. Poberaj, P. Günter, C. Boudon, J.-P. Gisselbrecht, M. Gross, U. Jonas, H. Ringsdorf, *Adv. Mater.* **1997**, *9,* 339–343.

[4] a) T. Ito, H. Shirakawa, S. Ikeda, *J. Polym. Sci. Polym. Chem. Ed.* **1974**, *12*, 11; b) T. Ito, H. Shirakawa, S. Ikeda, *Polymer. J.* **1971**, *2*, 231.

[5] a) G. Wegner, *Z. Naturforsch B* **1969**, *24*, 824; b) *Polydiacetylenes* (Eds.: D. Blood, R. R. Chance), Martinus Nijhoff, Dordrecht, **1985**, and references therein; c) S. Okada, H. Matsuda, H. Nakanishi, in *Polymeric Materials Encyclopedia* (Ed.: J. C. Salomone), CRC Press, Boca Ranton, FL, **1996**, p. 8393 and references therein; d) D. J. Sandman, *Trends Polym. Sci.* **1994**, *2*, 44; e) *Polydiacetylenes*, (Ed: H. J. Cantow), Springer, Berlin, **1984**, and references therein.

[6] L. Gobbi, P. Seiler, F. Diederich, *Angew. Chem.* **1999**, *111*, 740–743; *Angew. Chem. Int. Ed.* **1999**, *38*, 674–678.

[7] a) A. E. Reed, R. B. Weinstock, F. Weinhold, *J. Chem. Phys.* **1985**, *83*, 735; b) A. E. Reed, L. A. Curtiss, F. Weinhold, *Chem. Rev.* **1988**, *88*, 899; c) J. P. Foster, F. Weinhold, *J. Am. Chem. Soc.* **1980**, *102*, 7211; d) T. K. Brunck, F. Weinhold, *J. Am. Chem. Soc.* **1979**, *101*, 1700; e) A. E. Reed, F. Weinhold, *J. Chem. Phys.* **1985**, *83*, 1736; f) F. Weinhold, J. E. Carpenter in *The Structure of Small Molecules and Ions* (Eds.: R. Naaman, Z. Vager), Plenum, **1988**, p. 227.

[8] a) A. E. Reed, P. von R. Schleyer, *J. Am. Chem. Soc.* **1987**, *109*, 7362; b) A. E. Reed, P. v. R. Schleyer, *J. Am. Chem. Soc.* **1990**, *112*, 1434; c) U. Salzner, P. v. R. Schleyer, *Chem. Phys. Lett.* **1992**, *190*, 401; d) U. Salzner, P. von R. Schleyer, *J. Am. Chem. Soc.* **1993**, *115*, 10231; e) U. Salzner, P. von R. Schleyer, *J. Org. Chem.* **1994**, *59*, 2138.

[9] E. D. Glendening, R. Faust, A. Streitwiesser, K. P. C. Vollhardt, F. Weinhold, *J. Am. Chem. Soc.* **1993**, *115*, 10952–10957.

[10] A. Streitwiesser, *Molecular Orbital Theory for Organic Chemists*, Wiley, New York, **1961**.

[11] Y. Mo, S. D. Peyerimhoff, *J. Chem. Phys.* **1998**, *109*, 1687–1997.

[12] a) A. J. Heeger, S. Kivelson, J. R. Schrieffer, W.-P. Su, *Rev. Mod. Phys.* **1988**, *60*, 781; b) M. Kertsz, *Adv. Quantum Chem.* **1982**, *15*, 161; c) R. Peierls in *Quantum Theory of Solids*, Oxford University Press, Oxford, **1954**; d) A. A. Ovchinnikov, I. I. Ukrainskii, G. F. Kvenstel, *Usp. Fiz. Nauk* **1972**, *108*, 81.

[13] a) S. Suhai, *Phys. Rev. B* **1995**, *51(23)*, 16553–16557; b) C. H. Choi, M. Kertesz, A. Karpfen, *J. Chem. Phys.* **1997**, *107*, 6712–6721.

[14] J. Anthony, A. M. Boldi, Y. Rubin, M. Hobi, V. Gramlich, C. B. Knobler, P. Seiler, F. Diederich, *Helv. Chim. Acta* **1995**, *78*, 13–45.

[15] R. R. Tykwinski, A. Hilger, F. Diederich, H. P. Lüthi, P. Seiler, V. Gramlich, J.-P. Gisselbrecht, C. Boudon, M. Gross, *Helv. Chim. Acta* **2000**, 83, 1484–1508.

[16] A. Hilger, J.-P. Gisselbrecht, R. R. Tykwinski, C. Boudon, M. Schreiber, R. E. Martin, H. P. Lüthi, M. Gross, F. Diederich, *J. Am. Chem. Soc.* **1997**, *119*(9), 2069–2078.

[17] B. Ma, H. M. Sulzbach, Y. Xie, H. F. Schaefer, *J. Am. Chem. Soc.* **1994**, *116*, 3529–3538.

[18] M. Trætteberg, H. Hopf, *Acta Chem. Scand.* **1994**, *48*, 989–993.

[19] W. J. Hehre, R. Ditchfield, J. A. Pople, *J. Chem. Phys.* **1972**, *56*, 2257.

[20] T. H. Dunning, Jr., *J. Chem. Phys.* **1990**, *92*, 551; b) A. K. Wilson, T. van Mourik, T. H. Dunning, Jr., *J. Mol. Struct.* **1996**, *388*, 339.

[21] R. G. Parr, W. Yang, *Density Functional Theory of Atoms and Molecules*, Oxford University Press, New York, **1989**.

[22] a) A. D. Becke, *J. Chem. Phys.* **1992**, *96*, 2155–2160; b) A. D. Becke, *J. Chem. Phys.* **1993**, *98*, 5648–5652; c) P. J. Stevens, F. J. Devlin, C. F. Chablowski, M. J. Frisch, *J. Phys. Chem.* **1994**, *98*, 11623–11627.

[23] A. D. Becke, *Phys. Rev. A* **1988**, *38*, 3098–3104.

[24] C. Lee, W. Yang, R. G. Parr, *Phys. Rev. B* **1988**, *37*, 785.

[25] *Ab Initio Molecular Orbital Theory* (Eds.: W. J. Hehre, L. Random, P. von R. Scheleyer, J. A. Pople), Wiley, New York, **1986**.

[26] a) A. D. Bacon, M. C. Zerner, *Theor. Chim. Acta* **1979**, *53*, 21; b) M. C. Zerner, *Metal-Ligand Interactions*, Kluwer Academic, Dordrecht, The Netherlands, **1996**, p. 493; c) M. C. Zerner, G. H. Loew, R. F. Kirchner, U. T. Mueller-Westerhoff, *J. Am. Chem. Soc.* **1980**, *102*, 589; d) J. C. Culberson, P. Knappe, N. Rösch, M. C. Zerner, *Theor. Chim. Acta* **1987**, *71*, 21; e) J. Ridley, M. C. Zerner, *Theor. Chim. Acta* **1973**, *32*, 111; f) J. Ridley, M. C. Zerner, *Theor. Chim. Acta* **1976**, *42*, 223;

  0947-6539/02/0818-4226 $ 20.00+.50/0

g) W. P. Anderson, T. Cundari, R. S. Drago, M. C. Zerner, *Inorg. Chem.* **1989**, *29*, 150; h) W. P. Anderson, T. Cundari, M. C. Zerner, *Int. J. Quantum Chem*. **1991**, *39*, 31.
[27] G. S. Tschumper, H. F. Schaefer, *J. Chem. Phys.* **1997**, *107*, 2529–2541.
[28] A. D. Becke, *J. Chem. Phys.* **1993**, *98*, 1372.
[29] M. J. Frisch, G. W. Trucks, H. B. Schlegel, G. E. Scuseria, M. A. Robb, J. R. Cheeseman, V. G. Zakrzewski, J. A. Montgomery, R. E. Stratmann, J. C. Burant, S. Dapprich, J. M. Millam, A. D. Daniels, K. N. Kudin, M. C. Strain, O. Farkas, J. Tomasi, V. Barone, M. Cossi, R. Cammi, B. Mennucci, C. Pomelli, C. Adamo, S. Clifford, J. Ochterski, G. A. Petersson, P. Y. Ayala, Q. Cui, K. Morokuma, D. K. Malick, A. D. Rabuck, K. Raghavachari, J. B. Foresman, J. Cioslowski, J. V. Ortiz, B. B. Stefanov, G. Liu, A. Liashenko, P. Piskorz, I. Komaromi, R. Gomperts, R. L. Martin, D. J. Fox, T. Keith, M. A. Al-Laham, C. Y. Peng, A. Nanayakkara, C. Gonzalez, M. Challacombe, P. M. W. Gill, B. G. Johnson, W. Chen, M. W. Wong, J. L. Andres, M. Head-Gordon, E. S. Replogle, J. A. Pople, Gaussian 98 (Revision A.7), Gaussian Inc., Pittsburgh PA, **1998**.
[30] E. D. Glendening, A. E. Reed, J. E. Carpenter, F. Weinhold, NBO 3.1.

Received: February 7, 2002 [F3861]